LETTER

doi:10.1038/nature21032

# PLA2G16 represents a switch between entry and clearance of Picornaviridae

Jacqueline Staring[1], Eleonore von Castelmur[1], Vincent A. Blomen[1], Lisa G. van den Hengel[1], Markus Brockmann[1], Jim Baggen[2], Hendrik Jan Thibaut[2], Joppe Nieuwenhuis[1], Hans Janssen[1], Frank J. M. van Kuppeveld[2], Anastassis Perrakis[1], Jan E. Carette[3] & Thijn R. Brummelkamp[1,4,5]

**Picornaviruses are a leading cause of human and veterinary infections that result in various diseases, including polio and the common cold. As archetypical non-enveloped viruses, their biology has been extensively studied[1]. Although a range of different cell-surface receptors are bound by different picornaviruses[2–7], it is unclear whether common host factors are needed for them to reach the cytoplasm. Using genome-wide haploid genetic screens, here we identify the lipid-modifying enzyme PLA2G16 (refs 8–11) as a picornavirus host factor that is required for a previously unknown event in the viral life cycle. We find that PLA2G16 functions early during infection, enabling virion-mediated genome delivery into the cytoplasm, but not in any virion-assigned step, such as cell binding, endosomal trafficking or pore formation. To resolve this paradox, we screened for suppressors of the Δ*PLA2G16* phenotype and identified a mechanism previously implicated in the clearance of intracellular bacteria[12]. The sensor of this mechanism, galectin-8 (encoded by *LGALS8*), detects permeated endosomes and marks them for autophagic degradation, whereas PLA2G16 facilitates viral genome translocation and prevents clearance. This study uncovers two competing processes triggered by virus entry: activation of a pore-activated clearance pathway and recruitment of a phospholipase to enable genome release.**

To identify picornavirus host factors, mutagenized HAP1 cells were infected with different picornaviruses. Gene-trap insertions mapped in resistant cell populations (Fig. 1a) were enriched for mutations in the respective entry receptors such as the poliovirus receptor (*PVR*, $n = 475$ independent mutations) (Fig. 1b–e, Extended Data Fig. 1a and Supplementary Tables 1–5). In addition, *PLA2G16*, a gene not linked to virus infection before, was identified as a common host factor. *PLA2G16* encodes a small phospholipase implicated in obesity[13] located on the same genomic locus as its homologues *RARRES3* and *HRASLS2*, which were not enriched for disruptive mutations (Extended Data Fig. 1b).

In line with the absence of *PLA2G16* in previous haploid screens (performed with other viruses)[14–18], cells carrying a gene-trap insertion in the *PLA2G16* locus specifically displayed resistance to picornaviruses (Fig. 1f). Resistance to virus infection could be overcome by expression of a *PLA2G16* cDNA, which required the catalytic site cysteine (Cys113) (Extended Data Fig. 1c), suggesting that enzymatically active PLA2G16 functions as an important host factor for infection. *PLA2G16* inactivation using CRISPR/Cas9 gene-editing in HAP1, HeLa, HEK293T and A549 cells led to poliovirus type 1 (PV1) resistance (Extended Data Fig. 1d, e and Supplementary Table 7), and deficiency of *PLA2G16* in HeLa cells resulted in resistance to enteroviruses (including rhinoviruses) as well as picornaviruses of the Cardiovirus genus (encephalomyocarditis virus (EMCV), Saffold virus) (Fig. 1g and Extended Data Fig. 1f).

We then generated *Pla2g16*-deficient mice (Extended Data Fig. 2a, b), previously reported to be resistant to diet-induced obesity[13] (Extended Data Fig. 2c, d). Fibroblasts from these Δ*Pla2g16* mice showed resistance to infection by coxsackievirus A10 (CV-A10, Extended Data Fig. 2e). Injecting 1-day-old pups intraperitoneally with CV-A10 ($n = 14$ wild type, $n = 12$ Δ*Pla2g16*) or CV-A4 ($n = 12$ wild type, $n = 8$ Δ*Pla2g16*) resulted in high levels of double-stranded viral RNA staining in muscle tissue; whereas only modest staining was observed in *Pla2g16*-knockout mice (Fig. 1h). Notably, although wild-type mice succumbed to infection and displayed symptoms such as paralysis (Fig. 1i), most Δ*Pla2g16* animals infected with CV-A10 or CV-A4 (9 out of 12, or 12 out of 12 pups, respectively) showed no signs of illness for the duration of the experiment (at least 18 days).

To study the role of PLA2G16 in the infection cycle, we used fluorescently labelled poliovirus (Cy5-PV1). Δ*PLA2G16* HeLa cells showed normal levels of plasma membrane binding and subsequent internalization, indicating that PLA2G16 is not required for receptor binding or uptake into cells (Extended Data Fig. 3a, b). Infection of Δ*PLA2G16* cells complemented with a green fluorescent protein (GFP)-tagged *PLA2G16* transgene resulted in the appearance of cytoplasmic foci. These foci were in proximity to the Cy5-PV1 signal (Fig. 2a and Supplementary Video 1) and their appearance was prevented by the capsid-binding antiviral drug pleconaril (Extended Data Fig. 3c). Given the proximity of the lipid-modifying enzyme PLA2G16 to incoming virions, we asked whether PLA2G16 functions in pore formation—the next step of the infection cycle.

Virus-induced pore formation enables the cellular uptake of the proteinaceous ribosome-inactivating toxin α-sarcin[19] (Fig. 2b). Notably, exposure of either wild-type or Δ*PLA2G16* HeLa cells to PV1 in combination with α-sarcin readily inhibits translation in both cell lines (Fig. 2c), indicating that PLA2G16 is not essential for membrane permeabilization.

Picornavirus replication involves the accumulation of intracellular membrane structures, which are used for RNA replication. Δ*PLA2G16* cells rarely contained these viral replication sites (Extended Data Fig. 3d), suggesting that PLA2G16 acts after pore formation but before or concurrently with replication. To address this, we infected wild-type cells with a DsRed-expressing PV1. This virus must replicate to produce detectable fluorescence. Although many wild-type cells showed fluorescence (Fig. 2d) that could be blocked with the replication inhibitor guanidine hydrochloride (GHL)[20], no fluorescence was observed after infection of Δ*PLA2G16* cells. However, direct transfection of the viral genome into the cells bypassed the requirement for PLA2G16, and led to the generation of viral progeny as in wild-type cells (Fig. 2d and Extended Data Fig. 3e, f), indicating that PLA2G16 is not required for viral RNA replication. Collectively, our data point

[1]Netherlands Cancer Institute, Plesmanlaan 121, 1066 CX Amsterdam, The Netherlands. [2]Virology Division, Department of Infectious Diseases and Immunology, Faculty of Veterinary Medicine, Utrecht University, Yalelaan 1, 3584 CL Utrecht, The Netherlands. [3]Department of Microbiology and Immunology, Stanford University School of Medicine, 299 Campus Drive, Stanford, California 94305, USA. [4]CeMM Research Center for Molecular Medicine of the Austrian Academy of Sciences, 1090 Vienna, Austria. [5]Cancer GenomiCs.nl (CGC.nl), Plesmanlaan 121, 1066 CX Amsterdam, The Netherlands.

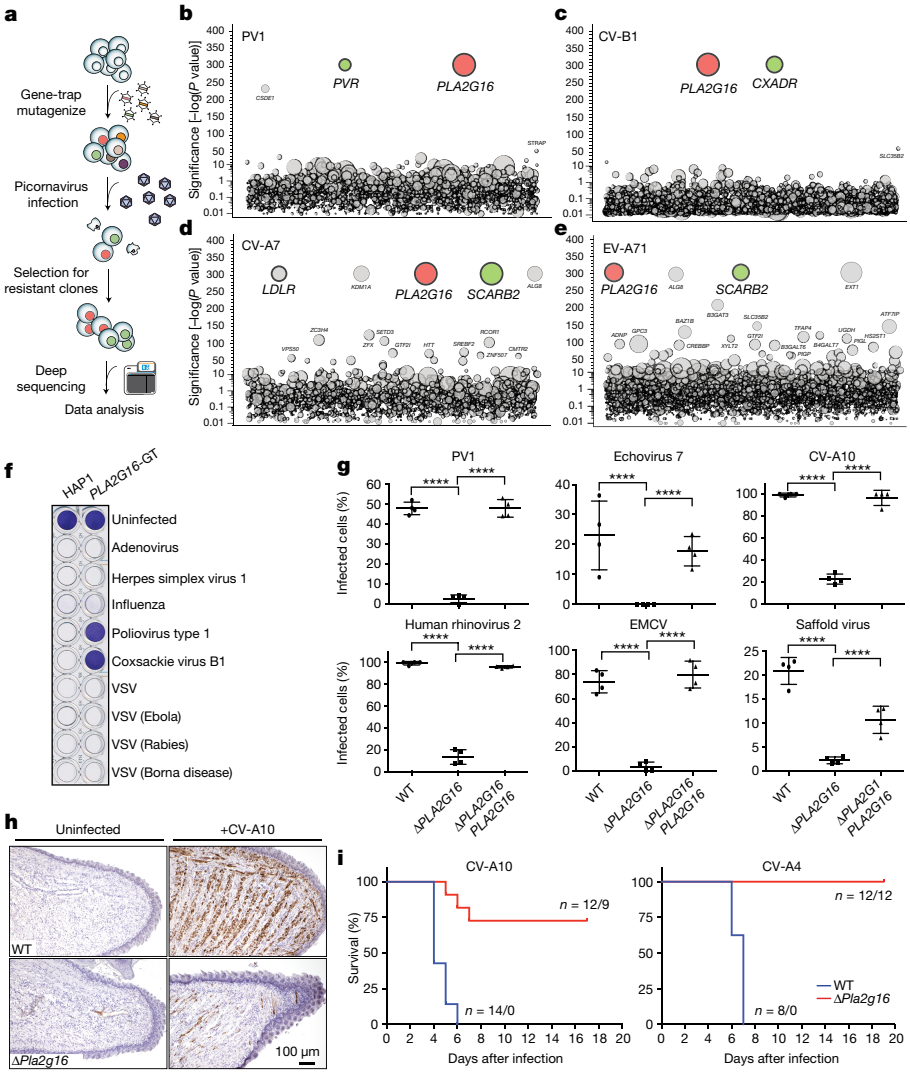


**Figure 1 | Identification of PLA2G16 as a host factor for picornaviruses.** **a**, Schematic overview of mutagenesis-based screen in haploid cells. **b**–**e**, Positive selection screens for picornavirus infection: PV1 (strain Sabin) (**b**) coxsackievirus B1 (CV-B1) (**c**), CV-A7 (**d**) and enterovirus A71 (EV-A71) (**e**). Each circle represents a gene, with size corresponding to the number of insertion sites per gene. The *y* axis indicates the significance of enrichment of several insertions in the affected gene compared to an unselected control. Genes were randomly distributed on the *x* axis. Coloured circles indicate known virus receptors and *PLA2G16*. **f**, Infection of wild-type (HAP1) and *PLA2G16* gene-trap insertion (*PLA2G16*-GT) cells with different viruses. Viable cells were stained using crystal violet ($n = 3$). **g**, Wild-type, Δ*PLA2G16* and Δ*PLA2G16* cells expressing *PLA2G16* cDNA were infected with picornaviruses. Cells were stained 8 h after infection with a double-stranded RNA (dsRNA) antibody, and infection efficiencies were quantified (mean ± s.d., $n = 4$, chi-square test, $^{****}P < 0.0001$). **h**, dsRNA staining of muscle tissue (tongue) of CV-A10 virus infection in wild-type and Δ*Pla2g16* mice. **i**, Kaplan–Meier graphs of infected wild-type and Δ*Pla2g16* mice exposed to CV-A10 (left) and CV-A4 (right). $P < 0.0001$ (log-rank test) for survival of Δ*Pla2g16* mice compared to wild type for both CV-A10 and CV-A4.

to a role for PLA2G16 in delivery of the viral genome to the cytoplasm from virions.

To gain additional insight into the phenotype of Δ*PLA2G16* cells, we designed a genetic suppressor screen to find mutants restoring virus susceptibility in Δ*PLA2G16* cells. We exposed mutagenized Δ*PLA2G16* HAP1 cells to PV1-DsRed, and used flow cytometry to select populations of DsRed-positive and -negative cells (Fig. 3a). For genes not affecting susceptibility to virus infection, gene-trap mutations should be recovered with comparable frequencies in both populations. However, the recovery of mutations in factors that affect virus susceptibility should be biased. Indeed, mutations in *PVR* were enriched in the DsRed-negative cell population (Extended Data Fig. 4a). Notably, in the DsRed-positive cell population, we identified a large number of genes involved in autophagy, membrane trafficking and glycosylation (Fig. 3b and Supplementary Table 6). This included the danger receptor *LGALS8* (also known as galectin-8), which was previously linked to autophagic clearance of intracellular bacteria[12]. This cytoplasmic lectin binds glycans of the external leaflet of host membranes, which become exposed when bacteria generate pores in the vacuole in which they reside, leading to the formation of autophagosomes. To determine whether a similar mechanism may affect viral infection, we expressed a GFP-tagged galectin-8 transgene (GFP–LGALS8) in Δ*PLA2G16* cells and exposed them to wild-type PV1 or coxsackievirus B1 (CV-B1). This led to the formation of cytoplasmic GFP–LGALS8 foci within minutes after infection (Extended Data Fig. 4b). Although the related galectin-3 (encoded by *LGALS3*) is recruited by adenovirus-induced membrane rupture, this has not been linked to viral restriction[21]. To test whether LGALS8 affects viral infection, we generated HeLa cells carrying single or double mutations in *PLA2G16*, *LGALS8* or the essential autophagy factor *ATG7* (Extended Data Fig. 4c). Exposure of these cells to PV1, CV-B1 or CV-B3–GFP demonstrated that loss of either *LGALS8* or *ATG7* restored virus susceptibility in Δ*PLA2G16* cells (Fig. 3c, d and Extended Data Figs 4d–f, 5a–c), suggesting that their resistance phenotype is at least in part a result of virus-induced LGALS8 recruitment.

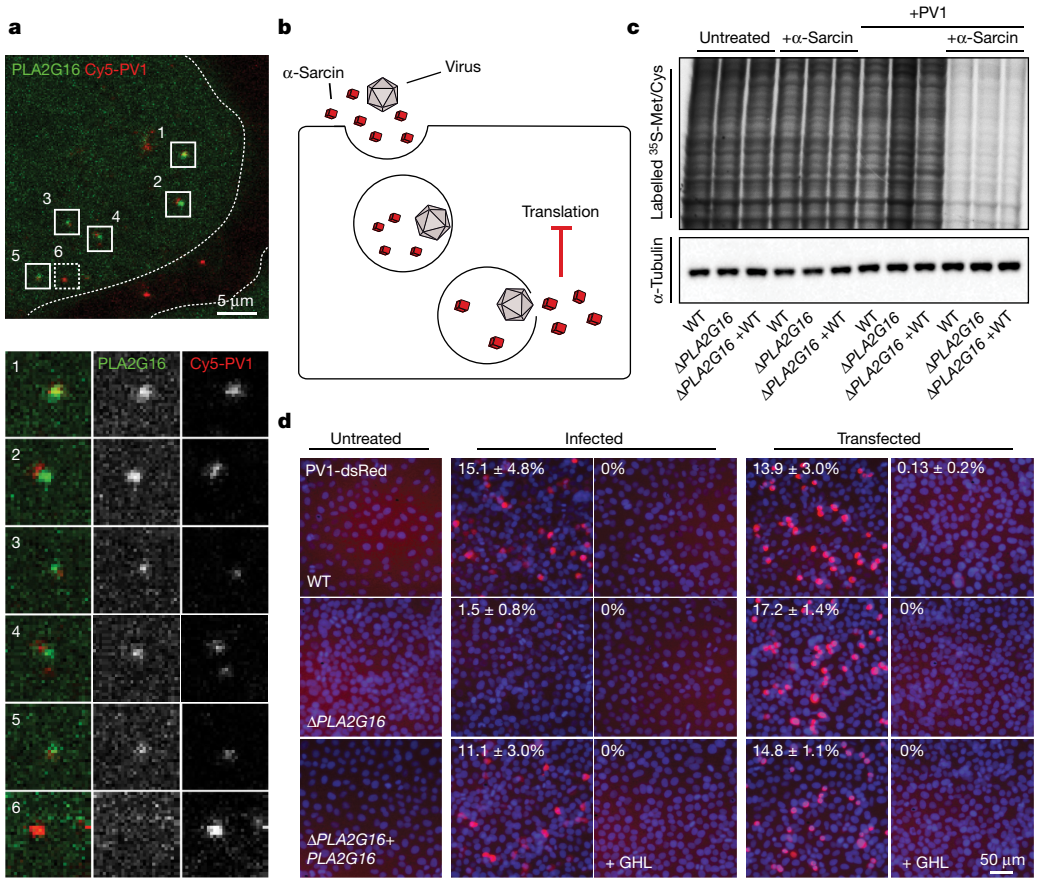


**Figure 2 | PLA2G16 functions after entry and before replication.** **a**, Localization of GFP–PLA2G16 (green) and Cy5-labelled PV1 (red; multiplicity of infection (MOI) value of ~10) in live HeLa cells 15 min after infection. Individual channels for different regions are shown. **b**, **c**, Schematic overview of pore-formation assay using α-sarcin (**b**), and a pore-formation assay with co-incubation of PV1 and α-sarcin (**c**). Translation was measured using $^{35}$S-methionine/cysteine-labelled incorporation. α-Tubulin served as loading control. For gel source data, see Supplementary Fig. 1. WT, wild type. **d**, Infection or transfection of PV1-DsRed (red) in the indicated genotypes. Cells were transfected with the viral genome (RNA) and DsRed expression was compared to expression in cells infected with PV1-DsRed virions. Cells were counterstained with Hoechst33342 (blue) for DNA. Inhibition of replication using GHL (2 mM) indicated that viral replication was required for the detection of DsRed expression (percentage values denote mean ± s.d., $n = 3$).

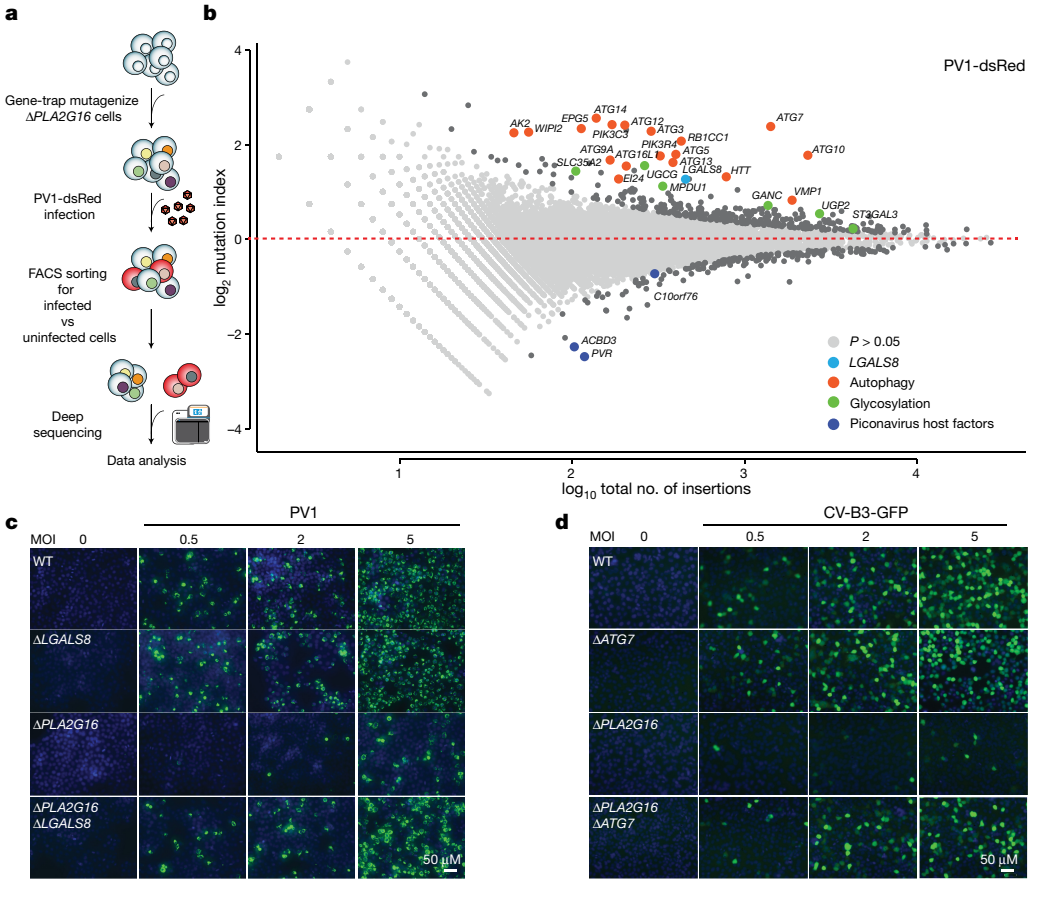


**Figure 3 | A suppressor screen identifies a pore-based restriction mechanism in Δ*PLA2G16* cells.** **a**, Schematic overview of PV1-DsRed suppressor screen using flow cytometric cell sorting of mutagenized haploid Δ*PLA2G16* cells. **b**, PV1-DsRed suppressor screen in Δ*PLA2G16* cells. Each dot represents a gene positioned on the *x* axis by the total amount of insertions per gene ($\log_{10}$). The *y* axis represents the mutation index (the relative number of integrations in the DsRed-high population divided by the relative number of integrations in the DsRed-low population for each individual gene). **c**, **d**, Galectin-8 (*LGALS8*) deficiency (**c**) or *ATG7* deficiency (**d**) restores virus susceptibility in Δ*PLA2G16* HeLa cells. Indicated genotypes were infected with an increasing amount of PV1 or CV-B3–GFP, and infected cells were detected using a dsRNA antibody or by measuring GFP expression, respectively ($n = 4$). Cells were counterstained with Hoechst33342 (blue) for DNA.

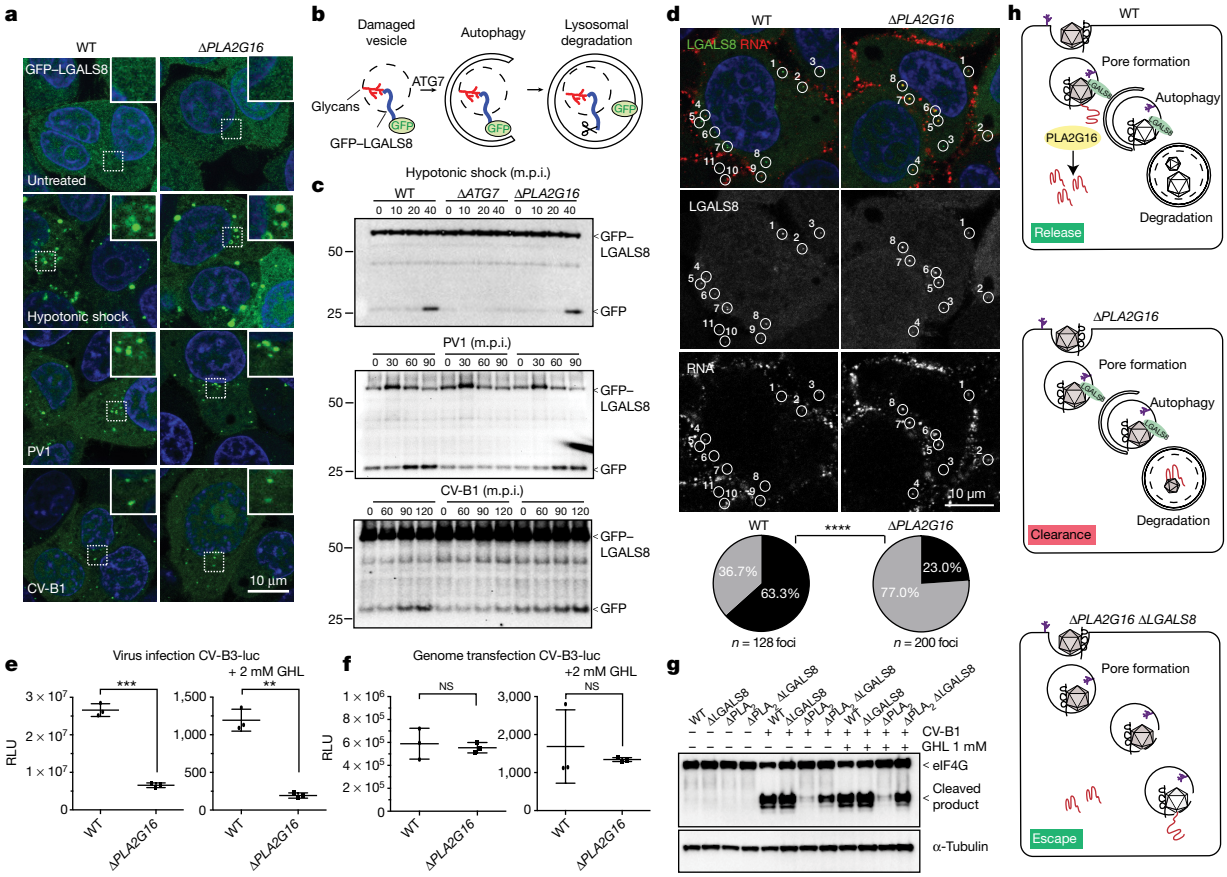


**Figure 4 | PLA2G16 facilitates genome dislocation from LGALS8 clusters and enables viral genome translation. a**, Wild-type and Δ*PLA2G16* HeLa cells expressing GFP-tagged galectin-8 (GFP–LGALS8; green) infected with PV1 and CV-B1 (MOI of ~20). Hypotonic shock serves to induce membrane damage. Insets represent magnifications of dashed boxes. **b**, Schematic overview of LGALS8 autophagic flux assay. **c**, Western blot analysis of autophagy-dependent GFP–LGALS8 cleavage during hypotonic shock (top) and infection with PV1 (middle) or CV-B1 (bottom) in the indicated genotypes. m.p.i., minutes post infection. **d**, *In situ* hybridization to detect PV1 RNA genomes (red) 30 min after infection in wild-type and Δ*PLA2G16* cells expressing GFP–LGALS8 (green). Circles represent examples of LGALS8 foci. In the pie charts (bottom), grey denotes LGALS8 foci positive for RNA, black denotes LGALS8 foci negative for RNA. $****P < 0.0001$, chi-square test, $n = 3$. **e**, Translation of incoming viral RNA using a CV-B3 expressing *Renilla* luciferase (CV-B3-luc). GHL served to block viral genome replication. $**P < 0.01$, $***P < 0.001$, unpaired two-sided Welch-corrected *t*-test, $n = 3$. RLU, relative light units. **f**, Transfection of CV-B3-luc RNA in wild-type versus Δ*PLA2G16* cells. $n = 3$; NS, not significant. **g**, Protein lysates of CV-B1-infected cells (MOI = 10, 2 h after infection) probed for eIF4G in indicated genotypes. GHL was added 30 min before infection. For gel source data, see Supplementary Fig. 1. **h**, Schematic model of the role of PLA2G16 during picornavirus entry.

As *LGALS8* and *PLA2G16* showed a genetic interaction, we investigated their connection. *PLA2G16* deficiency did not affect *LGALS8* recruitment by infection or pathogen-free (sterile) membrane damage induced by hypotonic shock[12] (Fig. 4a). Mutation of the carbohydrate-recognition domains (CRDs) of LGALS8 suggested that binding of host glycans to the N-terminal CRD trigger virus-induced LGALS8 recruitment, similar to bacterial pathogens[12] (Extended Data Fig. 6a, b). As PLA2G16 formed foci in infected cells (Fig. 2a), we asked whether PLA2G16 responded to membrane damage. Notably, as observed for LGALS8, GFP–PLA2G16 formed distinct cytoplasmic foci when cells were exposed to hypotonic shock (Extended Data Fig. 7a, b), and this was independent of LGALS8 (Extended Data Fig. 7c). Similarly, lysosome rupture led to the recruitment of LGALS8 (ref. 12) and subsequent accumulation of GFP–PLA2G16 (Extended Data Fig. 8a–d). Importantly, LGALS8 recruitment to damaged endosomes or ruptured lysosomes did not require PLA2G16 and vice versa (Extended Data Fig. 8e, f). Also, the localization of PLA2G16 to incoming viruses was independent of LGALS8 (Extended Data Fig. 8g). We found that the hydrophobic C terminus of PLA2G16 is needed to respond to membrane damage, suggesting that PLA2G16 may detect membrane damage autonomously (Extended Data Fig. 8h).

To determine whether PLA2G16 affects LGALS8 function, we modified an assay to measure autophagic flux involving release of GFP from the autophagy protein LC3-GFP by lysosomal proteases[22,23] (Fig. 4b). Exposure of GFP–LGALS8-expressing cells to hypotonic shock, PV1 or CV-B1 resulted in the formation of LGALS8 foci (Fig. 4a and Extended Data Fig. 9a) and increased the amount of free GFP (Fig. 4c), which required the autophagic machinery. GFP cleavage occurred to the same extent in Δ*PLA2G16* cells (Fig. 4c), suggesting that the ability of LGALS8 to trigger proteolysis of associated molecules is not influenced by PLA2G16.

Because LGALS8 activity was unaffected by PLA2G16, we followed the fate of the viral genome using LGALS8 as a tool to mark virions that have formed pores. In wild-type and Δ*PLA2G16* cells, viral genomes were initially detected at the plasma membrane (Extended Data Fig. 9b), which internalized at later time points (Extended Data Fig. 9c). In wild-type cells, most GFP–LGALS8 foci did not contain viral genomes (Fig. 4d). The opposite was observed in Δ*PLA2G16* cells, in which most LGALS8 foci did contain viral genomes. Crucially, this suggests that PLA2G16 facilitates the displacement of the viral genome from LGALS8-positive vesicles, which may promote viral translation. To test this, we measured viral translation before replication. Indeed, Δ*PLA2G16* cells displayed decreased translation of a viral luciferase

transgene upon infection, regardless of replication inhibition (Fig. 4e), but, consistent with previous data, not upon transfection (Fig. 4f). As an indicator of viral protein production, we also measured the cleavage of eIF4G by 2A protease in infected cells. Consistently, eIF4G cleavage was attenuated in Δ*PLA2G16* cells even when virus replication was blocked (Fig. 4g and Extended Data Fig. 9d). Together, this suggests that PLA2G16 does not affect the detection or autophagic clearance of permeated endosomes by LGALS8, but stimulates cytoplasmic availability of the viral genome to enable viral protein synthesis and subsequent replication (Fig. 4h).

In conclusion, we describe two membrane-linked mechanisms with opposing roles during picornavirus infection. The relocalization of PLA2G16 after membrane perturbation suggests that it may act as a cellular sensor of membrane damage at sites of virus entry. Its function may resemble a strategy used by parvoviruses carrying a capsid-linked $PLA_2$ to enable endosomal escape[24,25]. Similarly, PLA2G16 could be involved in initiating pore formation, increasing pore size, or in maintaining pores for genome delivery. Alternatively, modifying the membrane to which the capsid is anchored may alter membrane curvature and create forces towards the RNA-containing capsid, facilitating genome release. Remarkably, the 2A proteins of certain picornaviruses (for example, Aichivirus, parechovirus, and avian encephalomyelitis) are homologues of *PLA2G16* (ref. 26). This similarity, noted years ago, may now be related to a role for cellular PLA2G16 function in viral infection. We also demonstrate how membrane damage can trigger viral restriction. Viral restriction poses an intriguing impossibility: effective restriction mechanisms cannot exist; otherwise the affected virus would not exist. Thus, typically, restriction mechanisms are inactive in the host or cell type in which the virus replicates, or counteracted by viral factors. Ironically, however, here a cellular factor counters the restriction mechanism, posing intriguing questions on the co-evolution of these two processes.

**Online Content** Methods, along with any additional Extended Data display items and Source Data, are available in the online version of the paper; references unique to these sections appear only in the online paper.

**Received 4 July; accepted 6 December 2016.**
**Published online 11 January 2017.**

1. Tuthill, T. J., Groppelli, E., Hogle, J. M. & Rowlands, D. J. Picornaviruses. *Curr. Top. Microbiol. Immunol.* **343,** 43–89 (2010).
2. Racaniello, V. R. & Baltimore, D. Cloned poliovirus complementary DNA is infectious in mammalian cells. *Science* **214,** 916–919 (1981).
3. Hofer, F. *et al.* Members of the low density lipoprotein receptor family mediate cell entry of a minor-group common cold virus. *Proc. Natl Acad. Sci. USA* **91,** 1839–1842 (1994).
4. Bergelson, J. M. *et al.* Isolation of a common receptor for Coxsackie B viruses and adenoviruses 2 and 5. *Science* **275,** 1320–1323 (1997).
5. Bergelson, J. M. *et al.* Decay-accelerating factor (CD55), a glycosylphosphatidylinositol-anchored complement regulatory protein, is a receptor for several echoviruses. *Proc. Natl Acad. Sci. USA* **91,** 6245–6248 (1994).
6. Nishimura, Y. *et al.* Human P-selectin glycoprotein ligand-1 is a functional receptor for enterovirus 71. *Nat. Med.* **15,** 794–797 (2009).
7. Yamayoshi, S. *et al.* Scavenger receptor B2 is a cellular receptor for enterovirus 71. *Nat. Med.* **15,** 798–801 (2009).
8. Golczak, M. *et al.* Structural basis for the acyltransferase activity of lecithin:retinol acyltransferase-like proteins. *J. Biol. Chem.* **287,** 23790–23807 (2012).
9. Pang, X. Y. *et al.* Structure/function relationships of adipose phospholipase $A_2$ containing a Cys-His-His catalytic triad. *J. Biol. Chem.* **287,** 35260–35274 (2012).
10. Uyama, T. *et al.* The tumor suppressor gene H-Rev107 functions as a novel $Ca^{2+}$-independent cytosolic phospholipase $A_{1/2}$ of the thiol hydrolase type. *J. Lipid Res.* **50,** 685–693 (2009).
11. Uyama, T. *et al.* Regulation of peroxisomal lipid metabolism by catalytic activity of tumor suppressor H-rev107. *J. Biol. Chem.* **287,** 2706–2718 (2012).
12. Thurston, T. L. M., Wandel, M. P., von Muhlinen, N., Foeglein, A. & Randow, F. Galectin 8 targets damaged vesicles for autophagy to defend cells against bacterial invasion. *Nature* **482,** 414–418 (2012).
13. Jaworski, K. *et al.* AdPLA ablation increases lipolysis and prevents obesity induced by high-fat feeding or leptin deficiency. *Nat. Med.* **15,** 159–168 (2009).
14. Carette, J. E. *et al.* Haploid genetic screens in human cells identify host factors used by pathogens. *Science* **326,** 1231–1235 (2009).
15. Carette, J. E. *et al.* Ebola virus entry requires the cholesterol transporter Niemann-Pick C1. *Nature* **477,** 340–343 (2011).
16. Jae, L. T. *et al.* Deciphering the glycosylome of dystroglycanopathies using haploid screens for lassa virus entry. *Science* **340,** 479–483 (2013).
17. Riblett, A. M. *et al.* A haploid genetic screen identifies heparan sulfate proteoglycans supporting rift valley fever virus infection. *J. Virol.* **90,** 1414–1423 (2015).
18. Pillay, S. *et al.* An essential receptor for adeno-associated virus infection. *Nature* **530,** 108–112 (2016).
19. Fernández-Puentes, C. & Carrasco, L. Viral infection permeabilizes mammalian cells to protein toxins. *Cell* **20,** 769–775 (1980).
20. Tolskaya, E. A. *et al.* Genetic studies on the poliovirus 2C protein, an NTPase. A plausible mechanism of guanidine effect on the 2C function and evidence for the importance of 2C oligomerization. *J. Mol. Biol.* **236,** 1310–1323 (1994).
21. Maier, O., Marvin, S. A., Wodrich, H., Campbell, E. M. & Wiethoff, C. M. Spatiotemporal dynamics of adenovirus membrane rupture and endosomal escape. *J. Virol.* **86,** 10821–10828 (2012).
22. Gao, W., Ding, W. X., Stolz, D. B. & Yin, X. M. Induction of macroautophagy by exogenously introduced calcium. *Autophagy* **4,** 754–761 (2008).
23. Hosokawa, N., Hara, Y. & Mizushima, N. Generation of cell lines with tetracycline-regulated autophagy and a role for autophagy in controlling cell size. *FEBS Lett.* **580,** 2623–2629 (2006).
24. Zádori, Z. *et al.* A viral phospholipase $A_2$ is required for parvovirus infectivity. *Dev. Cell* **1,** 291–302 (2001).
25. Dorsch, S. *et al.* The VP1 unique region of parvovirus B19 and its constituent phospholipase A2-like activity. *J. Virol.* **76,** 2014–2018 (2002).
26. Hughes, P. J. & Stanway, G. The 2A proteins of three diverse picornaviruses are related to each other and to the H-rev107 family of proteins involved in the control of cell proliferation. *J. Gen. Virol.* **81,** 201–207 (2000).

**Supplementary Information** is available in the online version of the paper.

**Acknowledgements** The authors thank T. Sixma, L. Wessels, S. Nijman, G. Superti-Furga, W. Fischl, G. Casari and members of the Brummelkamp laboratory for discussions and reading of the manuscript; R. Bin Ali for assistance with generating knockout mice; and K. Kirkegaard and H. Ploegh for providing reagents. This work was supported by SNSF Fellowship PA00P3_145411 to E.V.C., and funding from the Cancer Genomics Center (CGC.nl), Nederlandse Organisatie voor Wetenschappelijk Onderzoek (NWO)–VIDI grant 91711316, European Research Council (ERC) Starting Grant (ERC-2012-StG 309634) to T.R.B. Work in the lab of F.J.M.V.K. was supported by NWO-VICI grant 91812628.

**Author Contributions** J.S., F.J.M.V.K., A.P., J.E.C. and T.R.B. were responsible for the overall design of the study, J.S. and J.E.C. carried out the host factor screens, V.A.B. performed the bioinformatics analysis, L.G.V.D.H. assisted in mouse experiments and the generation and characterization of knockout cell lines, M.B. performed the suppressor screen, J.N. contributed to microscopy analysis, H.J. performed electron microscopy studies, E.V.C. analysed *in vitro* experiments, J.B. and H.J.T. helped with preparation of virus stocks, luciferase assays and preparation of the EV-A71 screen. J.S. and T.R.B. wrote the manuscript, all authors commented on the manuscript.

**Author Information** Reprints and permissions information is available at www.nature.com/reprints. The authors declare competing financial interests: details are available in the online version of the paper. Readers are welcome to comment on the online version of the paper. Correspondence and requests for materials should be addressed to T.R.B. (t.brummelkamp@nki.nl).

**Reviewer Information** *Nature* thanks J. Bergelson, S. Lemon and the other anonymous reviewer(s) for their contribution to the peer review of this work.